Available online at www.sciencedirect.com
SCIENCE DIRECT®
Pergamon
Cement and Concrete Research 34 (2004) 139–148
CEMENT AND CONCRETE RESEARCH

Pore solution in alkali-activated slag cement pastes. Relation to the composition and structure of calcium silicate hydrate

F. Puertas*, A. Fernández-Jiménez, M.T. Blanco-Varela

Eduardo Torroja Institute, B.O.X. 19002, 28080 Madrid, Spain

Received 21 November 2002; accepted 18 July 2003

Abstract

In this work, the relationship between the composition of pore solution in alkali-activated slag cement (AAS) pastes activated with different alkaline activator, and the composition and structure of the main reaction products, has been studied. Pore solution was extracted from hardened AAS pastes. The analysis of the liquids was performed through different techniques: Na, Mg and Al by atomic absorption (AA), Ca ions by ionic chromatography (IC) and Si by colorimetry; pH was also determined. The solid phases were analysed by XRD, FTIR, solid-state ^{29}Si and ^{27}Al NMR and BSE/EDX.

The most significant changes in the ionic composition of the pore solution of the AAS pastes activated with waterglass take place between 3 and 24 h of reaction. These changes are due to the decrease of the Na content and mainly to the Si content. Results of ^{29}Si MAS NMR and FTIR confirm that the activation process takes place with more intensity after 3 h (although at this age, Q^2 units already exist). The pore solution of the AAS pastes activated with NaOH shows a different evolution to this of pastes activated with waterglass. The decrease of Na and Si contents progresses with time.

The nature of the alkaline activator influences the structure and composition of the calcium silicate hydrate formed as a consequence of the alkaline activation of the slag. The characteristic of calcium silicate hydrate in AAS pastes activated with waterglass is characterised by a low structural order with a low Ca/Si ratio. Besides, in this paste, Q^3 units are detected. The calcium silicate hydrate formed in the pastes activated with NaOH has a higher structural order (higher crystallinity) and contains more Al in its structure and a higher Ca/Si ratio than those obtained with waterglass.

Keywords: Alkali-activated cement; Pore solution; Calcium silicate hydrate (C-S-H); Microstructure

1. Introduction

Alkaline activation of vitreous blast furnace slag makes alternative cements that have important technical, economical and ecological advantages regarding ordinary Portland cements. Many authors have studied the alkali-activated slag cements (AAS) and concretes [1–5]. Recently, the knowledge of the influence of the different variables involved in the activation process on the development of strengths of AAS cements and mortars on their physical and mechanical properties (setting, shrinkage, strengths) and on the nature and structure of the main reaction products has advanced [6–9]. However, there are only few studies on the pore solution composition in the porous system of AAS pastes and concrete. In a recent work, Kim and Hong [10] studied the change of liquid concentration during hydration process of AAS pastes. They concluded that change depends on the nature of the activator and on the time.

In the present paper, the relationship between the compositions of pore solution in AAS pastes activated with different alkaline activator, and the composition and structure of the main reaction products, has been studied.

2. Experimental

A Spanish ground blast furnace slag was used. The chemical composition of the slag is shown in Table 1. The slag has 95% of vitreous content of and a specific surface of 460 $m^2\ kg^{-1}$. Two different activators were used: a $SiO_2{\cdot}nNa_2O{\cdot}mH_2O + NaOH$ ($SiO_2/Na_2O = 1.5$, pH = 13.10) mixture (waterglass solution) and a NaOH solution

* Corresponding author. Tel.: +34-913020440; fax: +34-913020700.
E-mail address: puertasf@ietcc.csic.es (F. Puertas).

0008-8846/$ – see front matter © 2003 Elsevier Ltd. All rights reserved.
doi:10.1016/S0008-8846(03)00254-0

Table 1
Chemical composition of blast furnace slag (wt.%)

CaO	SiO_2	Al_2O_3	Fe_2O_3	MgO	SO_3	S^{2-}	Na_2O	K_2O	Total
41.45	35.50	12.15	1.01	8.34	0.18	0.92	0.58	0.64	100.77

(pH = 13.6). The concentration of activator solutions was constant and equal to 4% Na_2O by mass of slag.

The activator/slag ratio used in paste preparations was 0.5. Pastes were cured in humid chamber (higher 95% RH) until the test time (3, 24, 48 h and 7 days). The extraction of pore solution from hardened AAS pastes was carried out using a device previously described by Barneyback and Diamond [11]. The steel is a special alloy (SAE-4340) able to resist discharge pressures (550 MPa).

Liquid analyses were carried out through different techniques: Na, Mg and Al by atomic absorption (AA), Ca ions by ionic chromatography (IC) and Si by colorimetry; pH was also determined. The activation process was stopped at the same ages by acetone/ethanol treatment, and the solid phases were analysed by different techniques.

Speciation and mineral water saturation calculation state of the brine solutions analysed after pore pressing test were calculated using the PHRQPITZ computer modelling program [12,13].

Solubility product of different phases used in this calculus was taken from the data base elaborated by Stronach [14]. In this data base, the author considers three C-S-H gels with Ca/Si ratios of 1.8, 1.1 and 0.8 (each of which is assigned a solubility value and a single continuous solubility curve).

X-ray diffractograms of powdered samples were recorded on a Philiphs diffractometer PW 1730 with CuKαradiation. The specimens were collected in the 2θ range 5–60° with a scanning rate of 2°/min, divergence slit = 1°, anti-scatter slit = 1° and receiving slit = 0.01 mm.

FTIR spectra were recorded with an ATIMATTSON apparatus, FTIR-TM series. Specimens were prepared by mixing 1 mg of the sample in 300 mg of KBr. The spectral analysis was performed in the range 4000–400 cm^{-1}, with a spectral resolution of 1 cm^{-1}.

Solid-state ^{29}Si and ^{27}Al NMR spectra were obtained with a Bruker MLS-400 spectrophotometer working at 79.49 and 104.26 MHz, respectively. ^{29}Si and ^{27}Al MAS NMR spectra were obtained after $\pi/2$ pulse excitations (4 μs) and 5 s of recycling delays. Spectra were recorded with MAS techniques, with sample spinning rates of 4 and 12 kHz. The number of scans was 800 and 200, respectively, for ^{29}Si and ^{27}Al spectra. Baseline distortions were eliminated after correction of dead time effects. ^{29}Si and ^{27}Al chemical shifts were reported with respect the tetramethylsilane (TMS) and 1M $AlCl_3{\cdot}6H_2O$ solutions, respectively. Spectral analyses were performed using the Winfit software package (Bruker). Intensity, position and line width of components were determined with a standard interactive least square method. Spectral simulations were within 2% of the observed spectra and estimated errors for chemical shifts and intensities lower than 0.2 ppm and 5%, respectively. In ^{29}Si cross polarization (CP) MAS experiments, contact time was 5 ms and recycling time 2 s.

Samples were examined through scanning electron microscopy and microanalysis after 7 days of curing, using backscattered electron imaging of polished surfaces. Samples were embedded into an epoxy resin, cut, polished and then coated with carbon. A JOEL JSM 5400 scanning electron microscope equipped with a solid-state backscattered detector and a LINK-ISIS energy dispersive (EDX) was used.

3. Results

Chemical composition of the extracted pore solution is presented in Table 2 and Fig. 1. Results show that the Na content in samples diminishes as the reaction time increases in the pastes activated with waterglass as much as in those activated with NaOH solution. To emphasize the low concentration of Mg and Ca ions in those pore solutions (see Table 2), although the anhydrous slag has in those ions a high content. The concentration of Al in all pore solutions stays in a very narrow range, located between 8.8 and 1.1 mmol l^{-1}, neither affecting the reaction time nor the activator nature. Finally, the concentration of Si in pore solution shows an evolution that is related with the nature of activator and with the reaction time. In AAS pastes with waterglass, the Si concentration at 3 h is very high (the activator contributes in an important amount of that Si); at 24 h, the Si content decreases abruptly (seven times the concentration at 3 h), then gradually, this decrease continues as the reaction time increases. In AAS paste with NaOH, after the first 3 h, there is a descent of the Si content in the pore solution. These concentrations are lower than those obtained in the corresponding pastes activated with waterglass.

According to thermodynamic calculations, all brine solutions are oversaturated in grossular (C_3AS_3), several terms of the hydrogarnet solid solution, gehlenite hydrate and C_3AH_6. The pore solution extracted at 7 days from paste activated with NaOH was not oversaturated in those two last phases.

In relation to the liquids extracted from pastes activated with NaOH at 3 h, the solution was also oversaturated in

Table 2
Chemical analyses of pore solutions extracted from AAS (mmol l^{-1})

Sample	Na	Mg	Ca	Al	Si	pH
N-3 h	$26{\cdot}10^2$	–	0.51	5.2	39.1	13.90
N-24 h	$22{\cdot}10^2$	–	0.39	8.8	28.4	13.74
N-48 h	$20{\cdot}10^2$	–	0.36	6.7	14.2	13.71
N-7 d	$18{\cdot}10^2$	0.01	0.21	4.8	7.1	13.73
W-3 h	$21{\cdot}10^2$	–	0.35	5.9	2243.3	13.26
W-24 h	$15{\cdot}10^2$	–	0.41	1.1	323.9	13.70
W-48 h	$13{\cdot}10^2$	–	0.37	2.9	181.5	13.42
W-7 d	$12{\cdot}10^2$	0.1	0.31	3.7	74.7	13.51

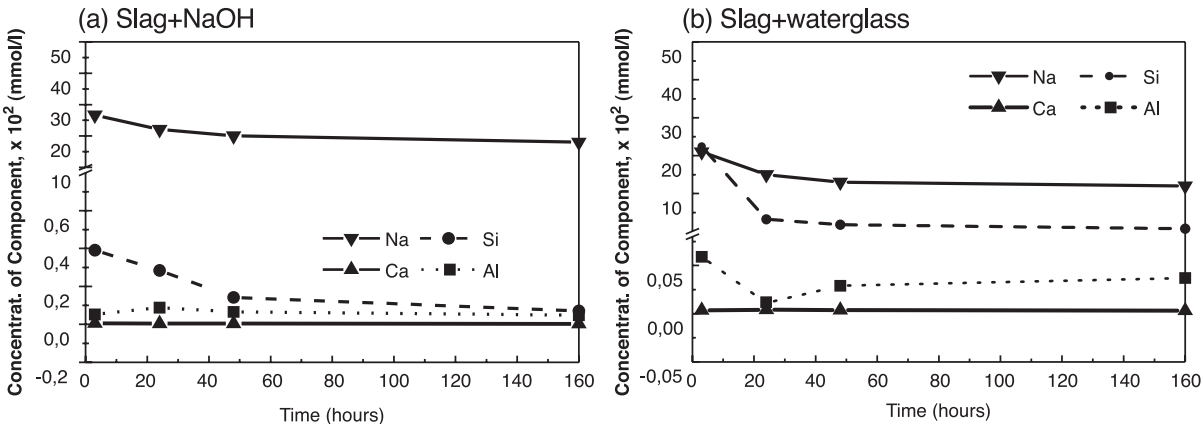

Fig. 1. Analytical results.

portlandite, C-S-H (1,8) gel, C-S-H (1,1) gel and C_4AH_{13}. After 1 day (solution at 24 h), the solution was not oversaturated in portlandite, and after 2 days, the solution was not oversaturated in any C-S-H gel. After 7 days, the solution was oversaturated in brucite and mainly in hydrotalcite.

As for solutions extracted from waterglass-activated samples, the solution at 3 h was not oversaturated in portlandite nor C_4AH_{13}, but in gibbsite, C-S-H (1,8) gel, C-S-H (1,1) gel and C-S-H (0,8) gel and a sodium silicoaluminate hydrate. After 1 day, the solution was neither oversaturated in gibbsite nor C-S-H (0.8) gel, and after 2 days, the solution remained oversaturated in both C-S-H (1,8) and C-S-H (1,1) gels, but with a lower oversaturation degree. After 7 days, the solution was oversaturated in brucite, hydrotalcite and C-S-H (1.1) gel.

The C-S-H gel solubility product is very difficult to calculate due to the variability in gel composition [15–17]. A number of models that make provision for two types of C-S-H gel are described in the literature [18–20]. The models proposed by Damidot and Glasser [20] and Stronach [14] are very similar, although in the latter, C-S-H gel (1.8) is metastable with respect to C-S-H gel (0.8) unless stabilized by adding C-S-H gel (1.1) or $Ca(OH)_2$. Despite this difference, the two models show rather similar solubility curve calculations.

As shown in Table 2, the pH of pore solutions experiences very small variations with the reaction time. In pastes activated with waterglass, the pH from the first 24 h is higher than that of the original solution. In pastes activated with NaOH, this phenomenon also takes place, but the difference between the pH of the original solution and the pH of the pore solution is smaller.

Mineralogical analysis carried out through XRD on the solid phases at 7 days of reaction shows some differences in the identified phases. In AAS paste activated with NaOH, phases identified were hydrotalcite ($Mg_6Al_2CO_3(OH)_{16}\cdot 4H_2O$), calcite ($CaCO_3$) and a semicrystalline calcium silicate hydrate (that has been identified through the more intense diffraction lines located at d($\mathring{A}$) = 12.5 and 3.07). In AAS pastes with waterglass, hydrotalcite was not detected and the identification of calcium silicate hydrate was more difficult

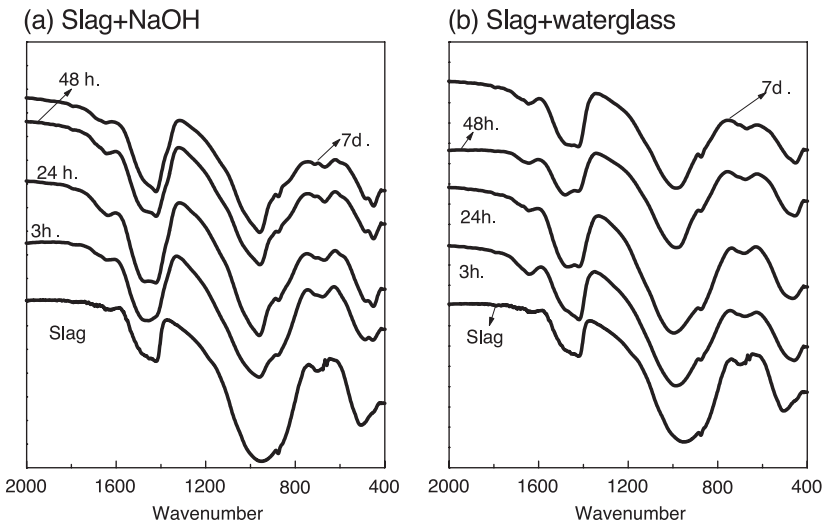

Fig. 2. FTIR spectra. (a) AAS pastes activated with NaOH, (b) AAS pastes activated with waterglass.

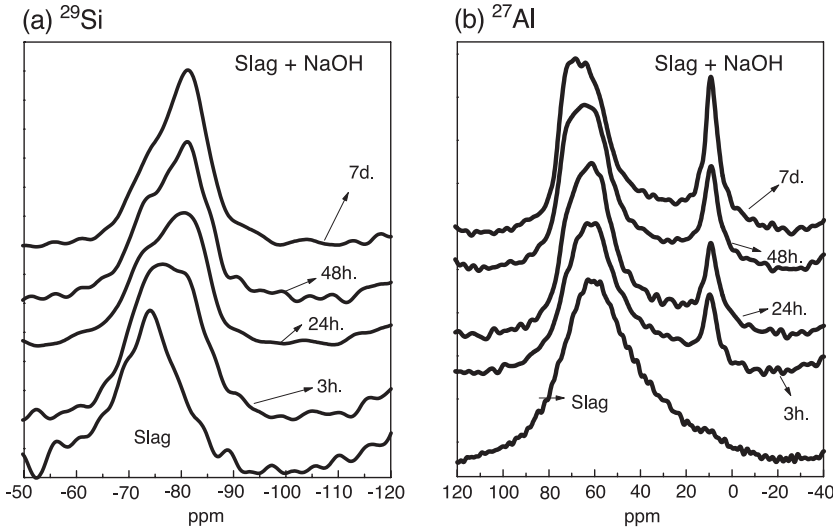

Fig. 3. ^{29}Si and ^{27}Al MAS NMR spectra of anhydrous slag and AAS pastes obtained by activation with NaOH.

than in the pastes activated with NaOH. Also, the presence of a calcium carbonate was detected.

FTIR spectra of the solid phases, at the different ages of curing, are shown in Fig. 2. The FTIR spectrum of anhydrous slag is formed by a broad band at 958 cm^{-1}, ascribed to ν_3(Si–O) stretching modes, and another located at 508 cm^{-1} assigned to ν_4(O–Si–O) bending modes of SiO_4 tetrahedra. In AAS pastes activated with NaOH, ν_3(Si–O) band shifts towards higher values (at 964 cm^{-1}) and ν_4(O–Si–O) band shifts towards lower values (at 450 cm^{-1}). These bands narrow as the reaction progresses. There is also a shoulder towards 1039 cm^{-1}, which has not yet been assigned. In the vibration region of Al–O bonds, from the first hours, a displacement of the wide band at 699 cm^{-1} in the anhydrous slag towards 660 cm^{-1} is observed. In the IR spectra of the pastes activated with waterglass (see Fig. 2b), a ν_3(Si–O) band shifts towards higher values (at 987 cm^{-1}) and ν_4(O–Si–O) band shifts towards lower values (at 457 cm^{-1}), which is also observed. As in previous spectra, these bands become sharper and more intense with reaction time. In these spectra, the absorption located at 1039 cm^{-1} is not observed. Also, the vibration of Al–O bonds at 699 cm^{-1} in the anhydrous slag moves towards 674 cm^{-1} in the activated pastes. In all pastes, the presence of calcium carbonates was confirmed, not only crystalline carbonates but also other noncrystalline ones.

^{29}Si and ^{27}Al MAS NMR spectra of anhydrous slag and AAS pastes obtained by activation with NaOH and waterglass appear in Figs. 3 and 4. The assignment of ^{29}Si NMR components was based on reported values obtained in aluminosilicates [21–24]. According to published data, peaks appearing between −73 and −78 ppm were assigned to Q^1 units, and peaks appearing between −83 and −85 ppm were assigned to Q^2 units. The substitution of Si by Al makes the signals to shift 3 or 5 ppm towards more positive values; taking into account this fact, the peak appearing at −81/−82 ppm was ascribed to Q^2(1Al). On the same basis, the peak appearing at −95/−97 ppm was attributed to the presence of Q^3(0Al) units, and the one at −91/−93 ppm to Q^3(1Al) units.

^{29}Si NMR spectrum of anhydrous slag shows a very wide asymmetric sign (~ 30 ppm) whose maximum appears at −74.05 ppm. Deconvolution on this spectrum, presented in Table 3, shows that this signal is the result of the sum of two components at −74.05 and −59.16 ppm. The main signal at −74 ppm (90%) is assigned by Richardson and Groves [25] to Q^0 units, and by Shilling et al. [21] to Q^1 units. The assignment to Q^1 units indicates that the silicate groups in

Table 3
^{9}Si and ^{27}Al MAS NMR data of anhydrous slag and AAS pastes activated with NaOH

	Slag	3 h	24 h	48 h	7 days	Assignment
^{29}Si	−59.2 ppm (6.2%)	−68.1 ppm (11.87%)	−69.0 ppm (13.27%)	−68.3 ppm (9.18%)	−69.2 ppm (6.95%)	Q^0
	−74.05 ppm (93.8%)	−73.6 ppm (31.56%)	−73.5 ppm (20.13%)	−73.5 ppm (21.38%)	−74.0 ppm (20.53%)	* Q^S (slag)
	–	−78.0 ppm (24.85%)	−78.0 ppm (23.23%)	−78.0 ppm (24.16%)	−78.6 ppm (28.4%)	Q_1 (chain end)
	–	−81.9 ppm (25.22%)	−81.5 ppm (27.88%)	−81.5 ppm (30.20%)	−82.0 ppm (33.8%)	Q_2 (1Al)
	–	−85.09 ppm (6.50%)	−85.00 ppm (15.49%)	−85.0 ppm (15.08%)	−85.5 ppm (10.35%)	Q_2 (0Al)
^{27}Al	+60.8 ppm (81.6%)	+61.89 ppm (71.83%)	+62.50 ppm (71.83%)	+63.86 ppm (72.01%)	+64.84 ppm (66.52%)	Al_T
	+32.6 ppm (12.2%)	+30.00 ppm (13.49%)	+30.00 ppm (13.49%)	+30.00 ppm (11.49%)	+30.00 ppm (12.54%)	Al_P
	+10.0 ppm (6.2%)	+8.66 ppm (14.67%)	+8.66 ppm (14.67%)	+8.94 ppm (16.20%)	+8.79 ppm (20.95%)	Al_O

* Q^S (slag) = Q^0 by Richardson and Groves [25] or Q^1 by Shilling et al. [21].

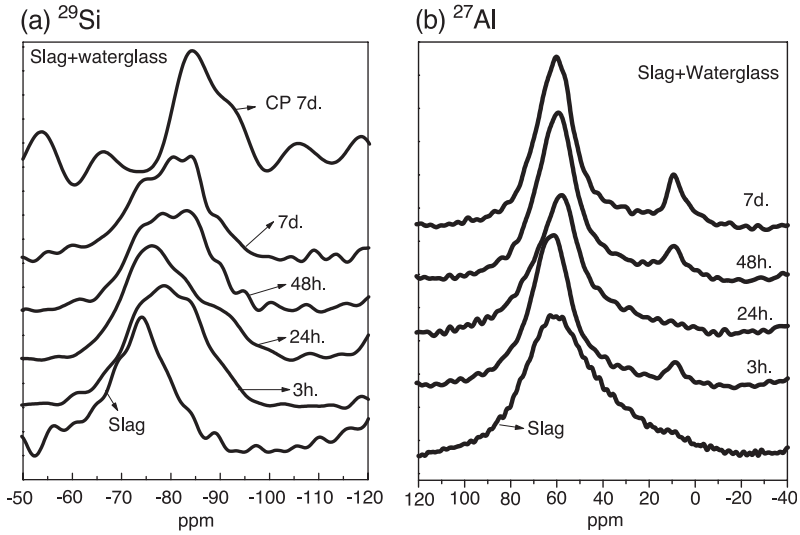

Fig. 4. ^{29}Si and ^{27}Al MAS NMR spectra of anhydrous slag and AAS pastes obtained by activation with waterglass.

slag are mostly organized in dimeric units. ^{27}Al MAS NMR spectrum of the slag shows a wide signal centred at +60 ppm, which is associated to the presence of tetrahedrally coordinated aluminum (Al_T = 81.6%, see Table 3) and two smaller components at +30 and +10 ppm due to pentahedrally (Al_P = 12.2%) and octahedrally coordinated aluminum (Al_O = 6.2%), respectively.

^{29}Si MAS NMR spectra from AAS pastes activated with NaOH solution display a wide signal formed by several maximums (Fig. 3a). As the reaction time increases, the maximum of that signal moves toward more negative values. The deconvolution of these spectra (see Table 3) shows the presence, from early ages, of Q^1 (chain end), Q^2(1Al) and Q^2 units. These units are associated to the formation of the main reaction product of the alkaline activation of slag, which is a calcium silicate hydrate with Al tetrahedrally incorporated in the structure. The percentage of these units, as well as the intensity of these signals, varies with reaction time (see Table 3), being in all cases the signal at −82 ppm, associated to Q^2(1Al) units, that of more intensity.

^{27}Al MAS NMR spectra from AAS pastes activated with NaOH solution is shown in Fig. 3b. A strong and broad asymmetric signal centred at +60 ppm formed by two components, one centred at +60 ppm associated to tetrahedral aluminum and another smaller centred at +30 ppm due to pentahedral aluminum, are observed. A third signal at +8/+9 ppm reveals the presence of a small amount of octahedrally coordinated aluminum.

^{29}Si CP MAS NMR spectrum of AAS pastes activated with waterglass at 7 days and ^{29}Si MAS NMR spectra of the same pastes at 3, 24, 48 h and 7 days are presented in Fig. 4a. The single-pulse ^{29}Si CP MAS NMR experiments inform about OH/H_2O groups near these environments. The absence of a peak at −74 ppm on the CP spectrum indicates that Al only substitutes Si in the central atom of linear chain in bridging tetrahedra. This result is in accordance with those obtained by Richardson et al. [22], Richardson and Cabrera [23] and Richardson and Groves [25].

In ^{29}Si MAS NMR spectra of AAS pastes with waterglass, several signals were detected. The maximum of the Si spectrum shifts towards more negative values as the reaction time increases. Data derived from deconvolution of this signal are given in Table 4. From these results, Q^1 (chain end), Q^2(1Al) and Q^2 units together with another signal of low intensity at −90/−91 ppm assigned to Q^3(1Al) units were detected.

Table 4
^{29}Si and ^{27}Al MAS NMR data of anhydrous slag and AAS pastes activated with waterglass

	Slag	3 h	24 h	48 h	7 days	Assignment
^{29}Si	−59.2 ppm (6.2%)	−68.5 ppm (8.24%)	−67.9 ppm (7.09%)	−67.3 ppm (7.15%)	−67.6 ppm (8.74%)	Q^0
	−74.05 ppm (93.8%)	−73.4 ppm (22.2%)	−73.8 ppm (31.69%)	−74.05 ppm (24.73%)	−73.5 ppm (20.95%)	* Q^S (slag)
		−78.2 ppm (25.01%)	−78.0 ppm (22.28%)	−78.0 ppm (18.27%)	−77.9 ppm (16.0%)	Q_1 (chain end)
		−82.0 ppm (17.5%)	−82.0 ppm (12.38%)	−82.0 ppm (18.27%)	−81.0 ppm (18.0%)	Q^2 (1Al)
		−85.0 ppm (17.04%)	−85.0 ppm (10.17%)	−85.0 ppm (21.06%)	−85.0 ppm (26.11%)	Q^2 (0Al)
		−90.7 ppm (9.92%)	−91.2 ppm (16.4%)	−90.6 ppm (10.53%)	−91.6 ppm (10.30%)	Q^3 (1Al)
^{27}Al	+60.81 ppm (81.6%)	+62.48 ppm (90.74%)	+59.73 ppm (89.20%)	+60.26 ppm (85.03%)	+60.81 ppm (82.57%)	Al_T
	+32.62 ppm (12.2%)	+30.00 ppm (5.17%)	+30.00 ppm (10.80%)	+30.00 ppm (7.13%)	+30.00 ppm (5.47%)	Al_P
	+10.02 ppm (6.2%)	+8.75 ppm (4.08%)		+9.22 ppm (7.84%)	+8.48 ppm (11.96%)	Al_O

* Q^S (slag) = Q^0 by Richardson and Groves [25] or Q^1 by Shilling et al. [21].

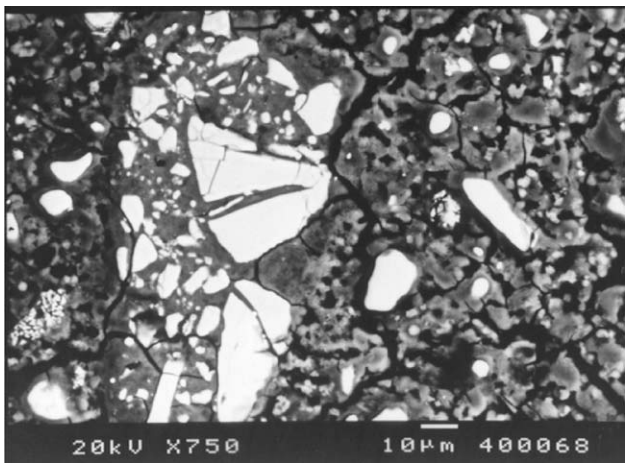

Fig. 5. BSE image of AAS pastes activated with NaOH (7 days).

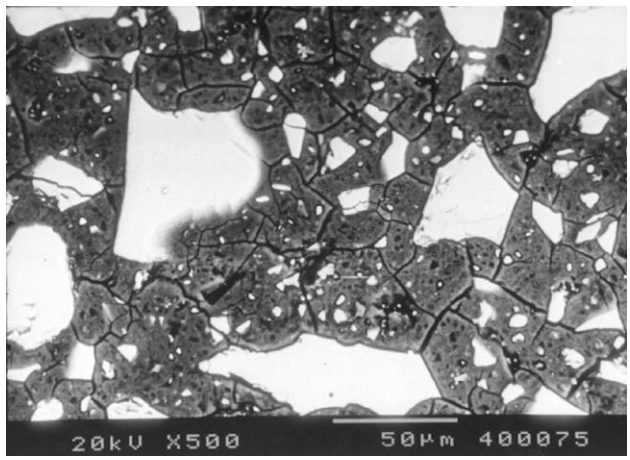

Fig. 6. BSE image of AAS pastes activated with waterglass (7 days).

^{27}Al MAS NMR spectra of AAS-activated pastes with waterglass are presented in Fig. 4b. Two signals were detected: one broad intense, asymmetric and centred around +60 ppm that was composed by two peaks at +60 ppm (Al_T) and +32 ppm (Al_P), and another signal less intense but sharper and centred at 7/8 ppm and ascribed to aluminum octahedrally coordinated (Al_O) (see Table 4).

The microscopical analysis carried out on activated pastes by BSE/EDX shows many unreacted slag particles. This microstructural analysis has confirmed that in all the pastes, the main reaction product is a calcium silicate hydrate. Some rings of reaction products of homogeneous texture and clear tonality are distinguished around of the unreacted slag grains in pastes activated with NaOH at 7 days. Similar textures to those described in areas that correspond to local reactions of large slag particles were also observed. In Fig. 5, a rest of large slag particles partially reacted are observed. Also in the same figure, another external morphology of reaction products, but with a more heterogeneous texture and a darker coloration, is observed. A detailed study of this dark area of reaction products permits to distinguish several tonalities of grey. The analyses carried out by EDX on the different textures described are displayed in Table 5.

AAS pastes activated with waterglass (7 days) present a high microcracking due to the tensions caused by the shrinkage experienced by the material (2). The cracks go through the matrix of reaction products and through the faces of the unreacted slag particles (see Fig. 6). In these pastes, the rings of reaction products observed in pastes activated with NaOH were not distinct. However, it was possible to identify reaction products with two different colors: one is clear and another darker. The analysis carried out by EDX on these particles is presented in the Table 5.

Table 5
Atomic ratios

Medium	No. of analysis	Ca/Si	Al/Ca	Mg/Ca	Al/Si	Na/Al
Unreacted slag	12	1.101	0.337	0.293	0.370	–
NaOH paste, clear	11	0.905	0.441	0.521	0.391	0.879
NaOH, dark	20	0.9239	0.484	0.664	0.427	0.94
Waterglass paste, clear	19	0.782	0.332	0.390	0.248	0.272
Waterglass, dark	18	0.766	0.446	0.722	0.330	1.867

EDX analysis.

4. Discussion

The high concentrations of OH^- ions in the alkaline solutions used as activators of the slag (NaOH and waterglass, pH>13) allow breaking the Ca–O, Si–O and Al–O bonds on the surface of the glassy slag [26,27]. The dissolved species in water are in the form of Ca^{2+}, $[H_2SiO_4]^{2-}$, $[H_3SiO_4]^-$ and $[H_4AlO_4]^-$ [27]. When the concentrations of these species reach the product of solubility of the different solid compounds, they precipitate, generating the microstructure of the AAS pastes. The evolution of these dissolved species in the time gives information about the reactive process and the formation of products in this type of materials.

The hydration and activation of cementitious materials (cements, slags, etc.) are a slow process, which reach the equilibrium (if they do) at very old ages. Solutions and solids produced during hydration are not in equilibrium and evolve dissolving ionic species and re-precipitating different phases.

The most significant changes in the ionic composition of the pore solution of the AAS pastes activated with waterglass take place between 3 and 24 h of reaction. These changes become evident because of the decrease in the Na content, which could be justified by the precipitation of a sodium silico-aluminate hydrate (phase in that the pore solution at 3 h was oversaturated) and mainly in the Si content. The large Si concentration at 3 h of reaction in the pore solution resulted mainly from the activator used ($SiO_2{\cdot}nNa_2O{\cdot}mH_2O$ + NaOH). According to thermodynamic results, C-S-H gels with Ca/Si ratios of 0.8 could precipitate in the pore solution at 3 h. The study carried out by FTIR has demonstrated that at 3 h, some reaction

products are formed, although in small intensity, since ν_3(Si–O) stretching band of its IR spectrum shifts towards higher frequencies, with respect to the anhydrous slag. When applying to this spectrum the technique of elimination of the bands belonging to the unreacted slag, it could be observed how ν_3(Si–O) band appears at 1000–1010 cm^{-1}, while in the IR spectra of the activated pastes at 48 h and 7 days, that band is located around 990 cm^{-1}. These results coincide with those obtained in previous works [8] where it was proved that in the system of slag activated with waterglass, two types of calcium silicate hydrate are formed. An initial silicate is formed as a result of the condensation and precipitation of the Si from the waterglass and the Ca of the slag, and another one at later ages with a higher Ca/Si ratio. $Q^1/\Sigma Q^2$ ratio in paste at 3 h is lesser than those at 24 h (see Table 6), which confirms the formation at 3 h of an initial calcium silicate hydrate with a lower Ca/Si ratio.

From 24 h of reaction, Si concentration decreases abruptly, indicating that the precipitation of reaction products intensified. These results agree with those found by other authors through conduction calorimetric studies [28]; they proved that the calorimetric signals associated to the massive precipitation of reaction products as a result of the alkaline activation of the slag with waterglass ended before the first 24 h. From the thermodynamic data, the pore solutions at 24 and 48 h are oversaturated in C-S-H gel with Ca/Si ratios of 1.8 and 1.1; after 7 days of reaction, the solution remains oversaturated in C-S-H gel with Ca/Si ratios of 1.1. Results of ^{29}Si MAS NMR confirm that the activation process takes place with more intensity from 3 h. $Q^1/\Sigma Q^2$ ratio drops drastically from 24 h of reaction (see Table 6). The decrease of this ratio indicates of the formation of solid species with longer tetrahedral silicate chains.

The pore solution of the AAS pastes activated with NaOH shows an evolution with time different to the one described in pastes activated with waterglass. The decrease of the Na and Si contents is progressive in time. In these pastes, the activation process of the slag is faster [6]. Thermodynamic results indicate that portlandite and C-S-H gels with Ca/Si ratios of 1.8 and 1.1 could precipitate in the solution after 3 h of reaction, while no more portlandite will precipitate in the solution after 24 h of reaction, being possible the precipitation of both C-S-H gels with Ca/Si ratios of 1.8 and 1.1. After 2 and 7 days of test, solutions were not oversaturated in any C-S-H gel. Results obtained by FTIR and ^{29}Si and ^{27}Al MAS NMR confirm that reactive processes have already started at 3 h of reaction, although it intensifies after 24 h. In the IR spectra, a displacement of the ν_3(Si–O) band to higher frequencies (964 cm^{-1}) is observed from the first 3 h, indicating the formation of a calcium silicate hydrate. In the 24-h IR spectra, this band stays in the same frequency (opposite to what happened in the activated pastes with waterglass), and it became sharper as the reaction time increased. This indicates the formation of a calcium silicate hydrate with a more structural order (through XRD, the higher crystallinity of that calcium silicate hydrate was confirmed). $Q^1/\Sigma Q^2$ ratio (see Table 6) diminishes between 3 and 24 h, staying almost constant at longer ages.

As it was previously mentioned the eight solutions analysed remained oversaturated in gehlenite hydrate and in some terms of the solid solution C_3AH_6 and C_3AS_3, then it seems that most part of the aluminum from slag is dissolved with time and precipitates in form of calcium aluminate hydrates, being the oversaturation degree in such phases lower as time progress. Mg^{2+} ions were detected in solutions only after 7 days of test in both solutions (with NaOH and waterglass); also, those solutions were highly oversaturated in hydrotalcite. From these results, a low solubility of Mg from the slag in these media at early ages could be deduced.

The nature of the alkaline activator induces differences in the structure and composition of the calcium silicate hydrate formed as a consequence of the alkaline activation of the slag [29]. The results obtained by FTIR and XRD confirm the formation, in these activated pastes, of a semicrystalline calcium silicate hydrate. The largest displacement in the ν_3(Si–O) band of IR spectra of pastes activated with waterglass shows a higher polymerization of that calcium silicate hydrate than those formed at same age in the pastes activated with NaOH. Results from XRD indicate, at the same time, a larger structural order of this last calcium silicate hydrate.

The analysis of the deconvolution data from the ^{29}Si and ^{27}Al MAS NMR spectra, and the microstructural studies, shows some structural and compositional differences between the calcium silicate hydrate formed in both activated pastes. To establish those differences, we observe the spectra at 7 days, and the values of $Q^1/\Sigma Q^2$, Q^2(0Al)/Q^2(1Al) and $Q^3/\Sigma Q^1 + Q^2$ ratios. These values can be seen in Table 6.

4.1. $Q^1/\Sigma Q^2$ ratio

Calcium silicate hydrate formed in AAS pastes activated with waterglass has a $Q^1/\Sigma Q^2$ ratio lower than the one formed in AAS pastes with NaOH. That means that the

Table 6
Different ratios derived from ^{29}Si and ^{27}Al MAS RMN spectra of AAS pastes

	NaOH, 3 h	NaOH, 24 h	NaOH, 48 h	NaOH, 7 h	Water, 3 h	Water, 24 h	Water, 48 h	Water, 7 h
$Q^1/\Sigma Q^2$	0.78	0.536	0.533	0.64	0.72	0.998	0.46	0.36
Q^2 (0Al)/Q^2 (1Al)	0.26	0.555	0.499	0.306	0.97	0.82	1.15	1.45
$Q^3/\Sigma Q^1 + \Sigma Q^2$					0.17	0.36	0.18	0.17

former has a larger amount of Q^2 units, thus higher length of tetrahedral silicate chains. The silicon from the activator contributes to the formation of this silicate rich in Si. Results obtained by microanalysis confirm the lower Ca/Si ratio in AAS pastes with waterglass (see Table 5), with values around 0.7–0.8, while Ca/Si ratio in AAS pastes with NaOH has values around 0.9–1.0.

4.2. $Q^2(0Al)/Q^2(1Al)$ ratio

In activated pastes with NaOH, the value of this ratio is 0.31, and in those activated with waterglass, the value is 1.45. These values indicate that the calcium silicate hydrate formed when the activator is NaOH contains more aluminum in its structure than those corresponding to waterglass. These results obtained by NMR coincide with those obtained after analysis through EDX. The Al/Si ratio found by microanalysis in activated pastes with NaOH is higher [Al/Si (0.35–0.42)] than those obtained in pastes activated with waterglass [Al/Si (0.25–0.33)]. The substitution of Si by Al in tetrahedral positions in the silicate chains has already been pointed out by several authors, for slag cement systems [23] and in activated slag systems [21,22,29].

4.3. $Q^3/\Sigma Q^1+Q^2$ ratio

Q^3 units are identified in activated pastes with waterglass, which means there are tetrahedra of silicates forming cross-linked type structures. The percentage of Q^3 units is constant from 24 h regarding the sum of Q^1 and Q^2 ($Q^3/\Sigma Q^1+Q^2=0.17–0.18$). The Q^3 units are not identified in activated pastes with NaOH solution. The presence of these units Q^3 in AAS pastes has been determined in other previous works [29–31].

Several hypotheses are involved that explain the detection of more condensed species, Q^3 environments: (i) a carbonation of calcium silicate hydrate formed in AAS pastes would reduce the Ca/Si ratio of the gel phase and form more condensed species [32], (ii) the formation of sodium silicates (lamellar or zeolitic materials); however, no signals of these phases were detected in XRD and FTIR spectra [33], (iii) the formation of cross-linked type structures. From the analysis of Q^2(1Al) and Q^3(1Al) intensity, it can be deduced that an important part of Al_T is implicated in formation of this cross-linked structures that can connect neighbouring structural blocks [29], (iv) from the sodium silicate solution used as activator [34].

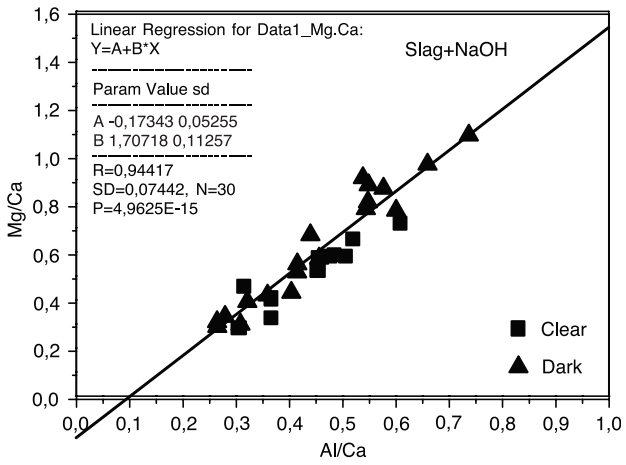

Fig. 7. Mg/Ca against Al/Ca ratio plot for analyses of AAS activated with NaOH.

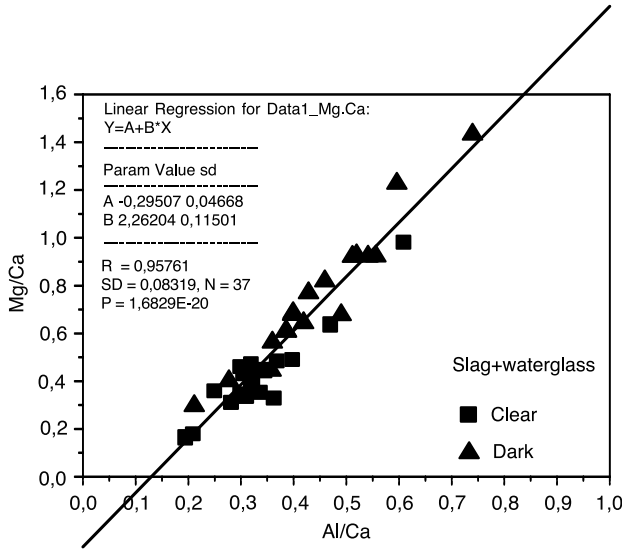

Fig. 8. Mg/Ca against Al/Ca ratio plot for analyses of AAS activated with waterglass.

Microstructural analyses carried out by BSE image revealed the presence in the matrix of several tonalities of grey. The clearest areas correspond to calcium silicate hydrate, which have different compositions as a function of the activator nature. The darkest areas have contents rich in Mg (see Table 6 and Mg/Ca ratio). Wang and Scrivener [35] studied alkali-activated cement pastes and concluded that a hydrotalcite-type phase is formed in the pastes activated with both NaOH and waterglass on a sub-micrometer scale in such a way that it cannot be distinguished in the SEM images. In Figs. 7 and 8, Mg/Ca ratios are plotted versus Al/Ca ratios for both NaOH and waterglass pastes, respectively. In both figures, the points are adjusted quite well to lines, existing some difference among clear and dark areas (the last ones have, in general, higher values of Mg/Ca and Al/Ca). If we extrapolate the straight line to Mg/Ca = 0 ratio, the values corresponding to Al/Ca are obtained that could be assigned only to calcium silicate hydrate. These values are in the case of the paste activated with NaOH 0.10 and 0.13 in the pastes activated with waterglass. These results confirm that the calcium silicate hydrate formed in the pastes activated with NaOH contains more Al in its structure and a higher Ca/Si ratio than those activated with waterglass.

5. Conclusions

The relationship existing between the compositions of the pore solution in AAS pastes, activated with different alkaline activator, and the composition and structure of the main reaction products, has been studied.

The most significant changes in the ionic composition of the pore solution of the AAS pastes activated with waterglass take place between 3 and 24 h of reaction. These changes are revealed by the decrease in the Na content and mainly in the Si content. Results of ^{29}Si MAS NMR and FTIR confirm that the activation process takes place with more intensity from 3 h (although at this age, Q^2 units already exist). $Q^1/\Sigma Q^2$ ratio diminishes drastically at the 24 h of reaction. The decrease of this ratio indicates of the formation a lengthening of tetrahedral silicate chains of solid species (a calcium silicate hydrate). Also, the ν_3(Si–O) stretching band of its IR spectrum shifts towards higher frequencies indicating a decrease in the Ca/Si ratio.

The pore solution of AAS pastes activated with NaOH show an evolution with time different to this pastes activated with waterglass. The decrease in Na and Si contents is progressive in time. The results obtained by FTIR and ^{29}Si and ^{27}Al MAS NMR confirm that the reactive processes have already started at 3 h of reaction, although it is intensified from 24 h.

The nature of the alkaline activator induces differences in the structure and composition of the calcium silicate hydrate formed as a consequence of the alkaline activation of the slag. When the activator is waterglass the calcium silicate hydrate is characterised by a low structural order with a low Ca/Si ratio. Likewise, in this paste, Q^3 units are detected. The calcium silicate hydrate formed in the pastes activated with NaOH has a higher structural ordering (higher crystallinity), contains more Al in its structure and a higher Ca/Si ratio than those obtained by the activation with waterglass.

Acknowledgements

Authors wish to thank the Ministerio de Ciencia y Tecnología (MCYT) for their support in the project MAT2001-1490. They also wish to thank Dr I. Sobrados and Dr J. Sanz for their collaboration in the RMN tests, and A. Gil and J.L. García for their help in the pore pressing tests.

References

[1] P. Krivenko, Alkaline cement: terminology, classification, aspects of durability, 10th ICCC (Goteborg), 1997, 4iv046.
[2] S.D. Wang, X.C. Pu, K.L. Scrivener, P.L. Pratt, Alkali-activated slag cement and concrete: a review of properties and problems, Adv. Cem. Res 7 (27) (1995) 93–102.
[3] F. Puertas, Cementos de escorias activadas alcalinamente: situación actual y perspectivas de futuro, Mater. Construcc. 239 (1995) 53–64 (Spanish).
[4] V. Glukhoskij, Y. Zaitsev, V. Pakhomow, Slag-alkaline cements and concretes-structures, properties, technologies and economical aspects of the use, Silic. Ind. 10 (1983) 197–200.
[5] B. Talling, J. Brandstetr, Present state and future of alkali-activated slag concretes. Fly ash, silica fuene, slag and natural pozzolans in concrete, Procee. 3rd Int. Conf. Trondheim, Norway, SP 114–174, CANMET/ACI, USA, 1989, pp. 1519–1545.
[6] A. Fernández-Jiménez, Cementos de escorias activadas alcalinamente: influencia de las variables y modelización del proceso. Doctoral Thesis, Universidad Autónoma de Madrid (2000) (Spanish).
[7] A. Fernández-Jiménez, J.G. Palomo, F. Puertas, Alkali-activated slag mortars. Mechanical strength behaviour, Cem. Concr. Res. 29 (1999) 1313–1321.
[8] A. Fernández-Jiménez, F. Puertas, Setting of alkali-activated slag cement. Influence of activator nature, Adv. Cem. Res 13 (3) (2001) 115–121.
[9] C. Shi, Strength, pore structure and permeability of alkali-activated slag mortars, Cem. Concr. Res. 26 (12) (1996) 1789–1799.
[10] J.C. Kim, S.Y. Hong, Liquid concentration changes during slag cement hydration by alkali activation, Cem. Concr. Res. 31 (2001) 283–285.
[11] R.S. Barneyback, S. Diamond, Expression and analysis of pore fluids from hardened cement pastes and mortars, Cem. Concr. Res. 11 (1981) 279–285.
[12] D.L. Parkhurst, D.C. Thorstenson, N.L. Plummer, PHREEQE—a computer program for geochemical calculations, U.S. Geol. Surv. (1980) (USGS-WRI-80-96).
[13] D.L. Parkhurst, G.W. Flemming, S.A. Dunkle, N.L. Plummer, PHRQPITZ—a computer program incorporating Pitzer's equation for calculation of geochemical reactions in brines, U.S. Geological Survey, Water Resources Investigations Report 88-4153, 1988.
[14] S.A. Stronach, Thermodinamic modeling and phase relations of cementitious systems, Thesis, University of Aberdeen, Scotland, 1996.
[15] F.P. Glasser, E.E. Lachawshi, D.E. Macphee, Compositional model for calcium silicate hydrate (C-S-H) gels their solubility and their free energies of formation, J. Am. Ceram. Soc. 70 (7) (1987) 481–485.
[16] R.R. Ramachandran, M.W. Grutzeck, Hydration of tricalcium silicate at pH fixed, 8th ICCC, Rio de Janeiro, vol. III, 1986, pp. 225–230.
[17] S.A. Jennings, Aqueous solubility relationship for two types of calcium silicate hydrate, J. Am. Ceram. Soc. 69 (1986) 614–618.
[18] E.M. Gartner, S.A. Jennings, Thermodynamics of calcium silicate hydrates and their solutions, J. Am. Ceram. Soc. 70 (1987) 743–749.
[19] A. Atkinson, C.F. Hearne, C.F. Knights, Aqueous chemistry and thermodynamic modeling of $CaO–SiO_2–H_2O$ gels, J. Chem. Soc. Dalton Trans. (1989) 2371–2379.
[20] D. Damidot, F.P. Glasser, Investigations of the $CaO–SiO_2–Al_2O_3–H_2O$ system at 25 °C by thermodynamic calculations, Cem. Concr. Res. 25 (1995) 22–28.
[21] P.J. Schilling, L.G. Butler, A. Roy, H.C. Heaton, ^{29}Si and ^{27}Al MAS-NMR of NaOH activated blast-furnace slag, J. Am. Ceram. Soc. 77 (9) (1994) 2363–2368.
[22] I.G. Richardson, A.R. Brough, G.W. Groves, C.M. Dobson, The characterisation of hardened alkali-activated blast-furnace slag pastes and the nature of the Calcium Silicate Hydrate (C-S-H), Cem. Concr. Res. 24 (5) (1994) 813–829.
[23] I.G. Richardson, J.G. Cabrera, The nature of C-S-H in model slag-cements, Cem. Concr. Compos. 20 (2000) 259–266.
[24] G. Engelhardth, D. Michel, High Resolution Solid State NMR of Silicates and Zeolites, Wiley, Chichester, UK, 1987.
[25] I.G. Richardson, G.W. Groves, The structure of the calcium silicate hydrate phases present in hardened pastes of white Portland cement/blast furnace slag blends, J. Mater. Sci 32 (1997) 4793–4802.
[26] I. Teoreanu, The interaction mechanism of blast-furnace slags with water, The role of the activating agents, Il Cemento 2 (1991) 91–97.
[27] C. Shi, Early hydration and microstructure development of alkali-activated slag cement pastes, in: H. Justness (Ed.), X Intern. Cong. Chem, Cem (Goteborg) vol. 3, 1997, 3ii099, 8, Trondheim, Norway.
[28] C. Shi, R.L. Day, A calorimetric study of early hydration of alkali-slag cements, Cem. Concr. Res. 25 (6) (1995) 91–97.

[29] A. Fernandez-Jiménez, F. Puertas, I. Sobrados, J. Sanz, Structure of calcium silicate hydrate formed in alkaline activated slag, Influence of the alkaline activator nature, J. Am. Ceram. Soc. (in press).
[30] A.R. Brough, A.A. Tkinson, Sodium silicate-based, alkali-activated slag mortars: Part I. Strength, hydration and microstructure, Cem. Concr. Res. 32 (2002) 865–879 (BRNO University of Technology, Czech Republic).
[31] A. Fernández-Jiménez, F. Puertas, I. Sobrados, J. Sanz, Structure of calcium silicate hydrate formed in alkali activated slag cement pates, in: V. Bílek, Z. Kersner (Eds.), Non-Traditional Cement and Concrete, 2002, pp. 29–41.
[32] A.R. Grimmer, Structural investigation of calcium silicate from ^{29}Si chemical shift measurements, in: P. Colombet, A.R. Grimmer (Eds.), Application of NMR Spectroscopy to Cement Science, Gordon and Breach Science Publishers, Amsterdam, 1994, p. 135.
[33] W. Wieker, C. Hübert, D. Heidemann, Recent results of solid-state NMR investigations and their possibilities of use in cement chemistry, 10th ICCC (Goterborg) vol. 1, H. Justness, Trondheim, Norway, 1997, 24 pp.
[34] D. Hoebbel, R. Ebert, Sodium silicate solution-structure, properties and problems, Z. Chem. 28 (2) (1988) 41–51.
[35] S.D. Wang, K.L. Scrivener, Hydration products of alkali-activated slag cement, Cem. Concr. Res. 25 (3) (1995) 561–571.